

LARGE DETECTORS FOR HADRON COLLIDERS:
EXPERIENCE AND FUTURE

Bernard Sadoulet
UAI Collaboration
CERN, Geneva, Switzerland

1. Introduction

In this talk, addressed mainly to accelerator physicists, we will describe the existing (and nearly existing) large detectors for hadron colliders (Section 2). From the experience with the CERN Sp \bar{p} S Collider, we will attempt to draw a lesson both in terms of physics (Section 3) and in terms of hardware capabilities (Section 4). We will then outline the main challenges for the near future (Section 5). And we will finally conclude that our present detectors may be the prototypes of a class of detectors for 20-40 TeV colliders.

No mention will be made of e^+e^- or ISR detectors, although the success of MARK I at SPEAR had a predominant influence on the design of collider detectors, and most of the techniques used have been developed at the ISR, PEP or PETRA.

2. Existing $p\bar{p}$ Detectors

2.1 General Principles

The aim of the experimental physicists working at a collider is to describe *individual* collisions in as much detail as possible. What are the types of particles produced? What is their charge, their angle of emission, their energy, etc.?

In order to approach that goal, they enclose the interaction point with concentric sets of detectors, each specialized in a particular task. The classical structure is to surround the beam pipe by a central detector which shows the trajectories of charged particles. If it is immersed in a magnetic field, it will allow the measurement of the momenta of the particles. Around it, shower counters will reconstruct the electromagnetic energy distribution. This electromagnetic calorimeter is itself surrounded by a hadron calorimeter measuring hadron energy. Outside, behind the shielding provided by the two calorimeters and perhaps additional iron, track-sensitive chambers measure emerging muons.

In this "Russian doll" arrangement, each particle type has a specific signature.

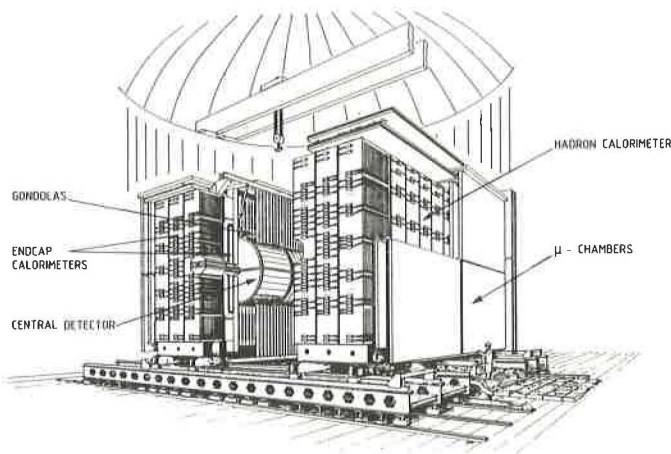


Fig. 1 Artist's view of the UA1 detector

A charged hadron will have its angles of emission and its momentum measured by the central detector. It will then initiate a fat shower, with a typical diameter of 20 cm (for 90% energy containment at shower maximum), starting usually late in the calorimeters.

An electron (or positron) will have its momentum measured in the central detector and its energy determined by the calorimeter. The two measurements should be compatible. The shower in the calorimeters has very striking characteristics. It starts early in the electromagnetic part and, if the electromagnetic calorimeter is deep enough, it dies before the hadronic calorimeter. The shower is very slim (typical diameter equal to 2 cm for 90% energy containment at shower maximum) and its position should agree with the extrapolation from the central detector.

A muon, on the other hand, should not have any interaction in the electromagnetic or the hadronic calorimeters. After depositing energy by dE/dx in these two detectors, it will emerge in the muon chambers. The measurement of angle and position in these chambers should agree with those extrapolated from the central detector.

A photon (either produced directly or from π^0 decay) will of course not leave any track in the central detector. In the electromagnetic calorimeter it will initiate a shower, which is very similar to that of an electron. In particular, it does not reach the hadron calorimeter.

A jet is a mixture of charged hadrons and π^0 's. Its charged component will be measured in the central detector and a superposition of fat and slim showers will be detected in the calorimeters.

Finally, high-energy colliders allow the study of weak interactions in which neutrinos are produced. Unfortunately, they do not have significant interactions with matter and the only way to detect them is by observing an imbalance of energy in the rest of the event. Since it is easy to lose energy along the beam pipe, missing transverse energy is used as a signature.

2.2 UA1

The UA1 detector¹ at the CERN Sp \bar{p} S Collider uses all these signatures. An artist's view, as shown in Fig. 1, allows identification of the various elements. Figure 2 gives a view along the beam, where the

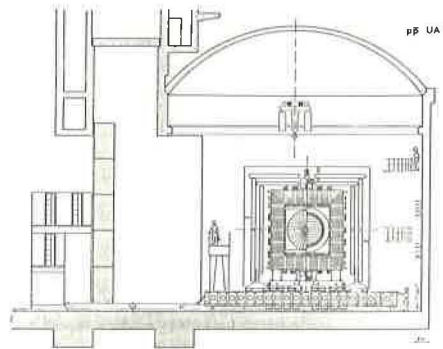


Fig. 2 UA1 detector as seen along the beam

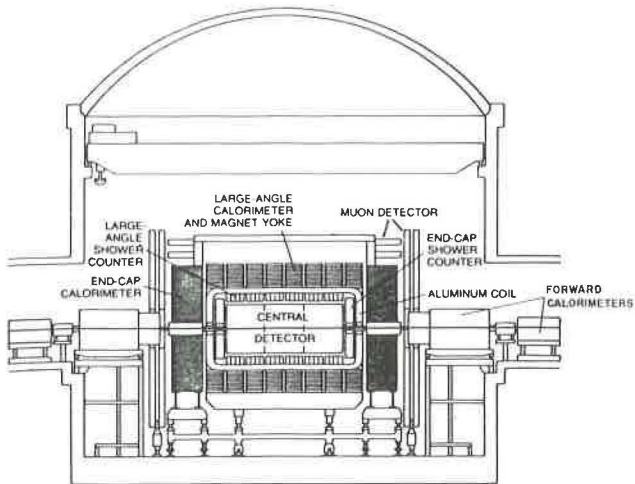


Fig. 3 Elevation view of UA1 detector

"Russian doll" structure can be recognized. An attempt to capture as much energy as possible leads to a complex structure in the forward directions as exemplified in Fig. 3.

2.3 UA2

The UA2 team at the CERN Sp \bar{p} S Collider searched for simplifications which cut the construction costs by roughly a factor of 2 with respect to the UA1 detector. The main emphasis² (Fig. 4) has been put on the central calorimeter, which has a tower structure and better segmentation in azimuth than UA1 (240 cells instead of 20 in the polar region 40°-140°). In order to make a compact device, no magnetic field is used in that region. The consequent loss of the power to reject pions when selecting electrons is partially

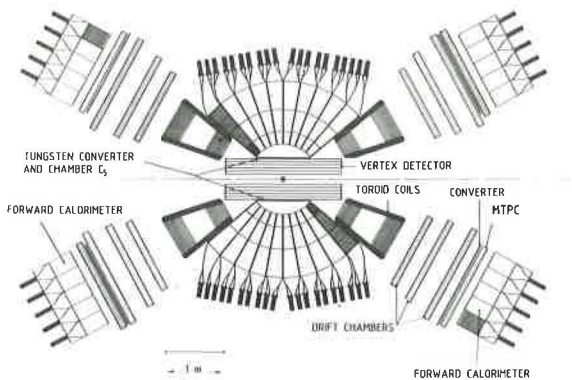


Fig. 4 The UA2 detector. It is rotationally symmetric around the beam.

compensated by a position detector (C5) locating the electromagnetic shower after 1.5 radiation lengths. In the polar region 20°-40° (140°, 160°) momentum measurement is provided by toroids, but no hadron calorimeter is instrumented. No measurement is attempted below 20°. Therefore, transverse energy can escape easily and ν detection capability is limited. No attempt is made to detect muons.

2.4 CDF

For Tevatron I at Fermilab, a general facility (the Collider Detector Facility³, CDF) is under design and construction. Figure 5 gives a general overview. The basic structure is the same as the UA1 detector, although the magnetic field is parallel to the beam and

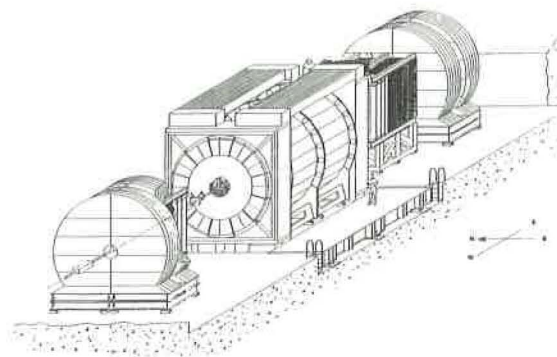


Fig. 5 Artist's view of the Fermilab CDF

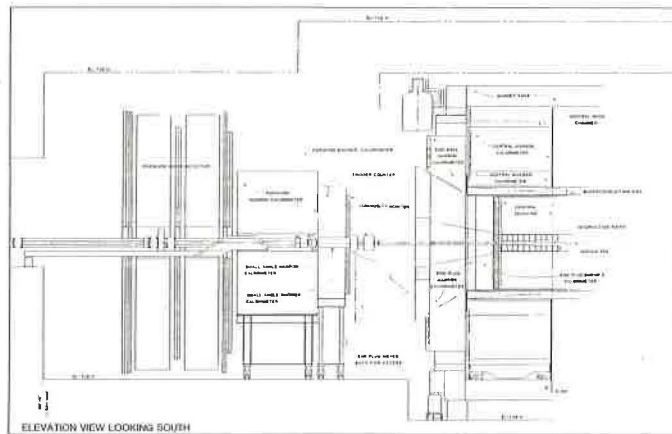


Fig. 6 Elevation view of half the CDF

some iron toroids allow measurement of the muons in the forward directions. Figure 6 shows the elevation view of half of the detector. The design of the central calorimeter is similar to that of UA2 with a tower structure of comparable segmentation.

3. What Have we Learned from the CERN Sp \bar{p} S Collider?

These two years of operation of the CERN Sp \bar{p} S Collider have deeply transformed our view of physics with high-energy hadron colliders.

3.1 Importance of Weak Interactions

For the first time weak interactions appear to play a major role in hadronic reactions. The discovery⁴ of the W (Fig. 7) and Z⁰ (Fig. 8) is a spectacular illustration. The top quark t, if it exists, will also decay via weak interaction, for instance in the reaction

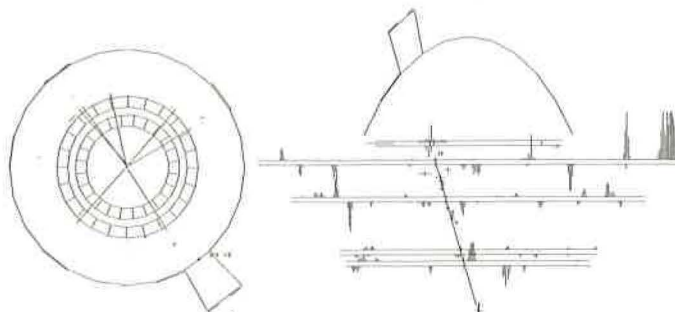


Fig. 7 A $W \rightarrow e\nu$ event as seen by the UA2 Collaboration

$$t \rightarrow b + e + \nu,$$

where the electron e and the neutrino ν have large transverse momentum (~ 10 GeV/c) with respect to the beauty quark b . It is therefore important for the detectors to be able to identify and measure well *charged leptons* (electrons and muons) and *neutrinos* with significant transverse energy, as they are a good signature of weak interactions. Moreover, the decay path may be sizeable (see Section 5.2).

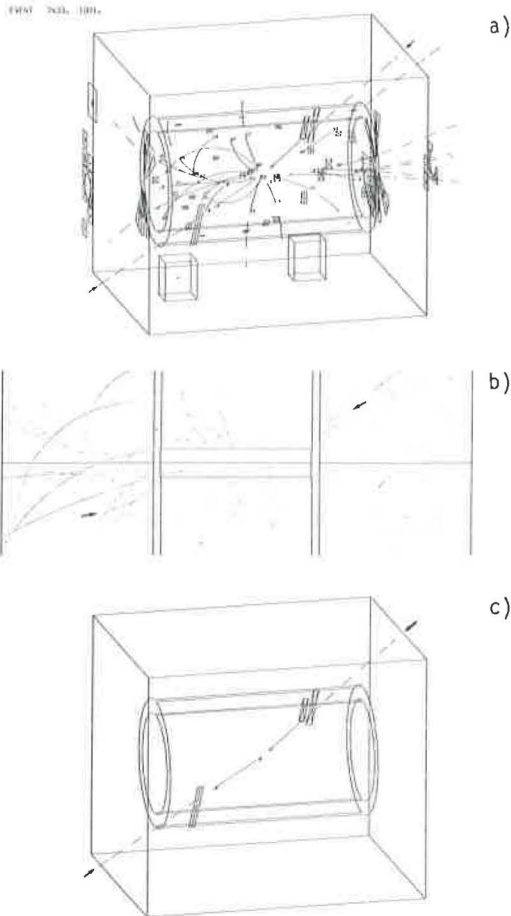


Fig. 8 A $Z^0 \rightarrow e^+e^-$ event as seen by the UA1 Collaboration. a) No threshold; b) Central detector raw digitizings. The electrons are indicated by arrows; c) $p_T > 2$ GeV/c in central detector, $E_T > 2$ GeV in calorimeter cells.

3.2 High-energy Hadron Colliders are Clean

In contrast with common expectations, hadron colliders are producing extremely clean events. As an example, we show in Figs. 8a and b a Z^0 event observed by UA1 with all tracks and all hits in the calorimeters. Obviously there are many low transverse energy particles which obscure the picture. However, as soon as a moderate threshold in transverse energy is imposed ($p_T > 2$ GeV/c in the central detector, $E_T > 2$ GeV in the calorimeter) only the two electrons from the Z^0 decay are left (Fig. 8c). Their transverse energy is of the order of 40 GeV.

This cleanliness of large transverse momentum events is quite general. These events are also the most interesting since they are believed to be due to the interactions of "elementary" constituents of the hadrons: quarks and gluons. Since their size is much smaller, they give rise to large-angle scattering. In

fact, high-energy hadron colliders can be considered as quark-quark or gluon-gluon or gluon-quark colliders (in 10^{-4} of the cases!) and in that respect quite complementary to e^+e^- machines.

Of course, the "evaporation" particles of low transverse momentum, which are essentially irrelevant, have to be filtered out. The above example shows the power of a *magnetic field* for that purpose.

3.3 Jets are the Interesting Objects

In quantum chromodynamics, it is believed that these quarks and gluons cannot escape from the interaction volume because they carry a forbidden quantum number ("colour"). They will "dress" themselves with surrounding quarks from the vacuum and manifest themselves as tight "jets" of hadrons. Such jets are indeed observed⁵.

Figure 9a shows a two-jet event in the UA1 detector (with a 1 GeV threshold). The "Lego plot" of Fig. 9b shows that the transverse energy deposition is indeed very concentrated in two polar angle regions back to back in azimuth. Figure 10 shows a UA2 event with three jets where presumably one of the scattered quarks or gluons has radiated an additional gluon in a process similar to that of bremsstrahlung in electrodynamics.

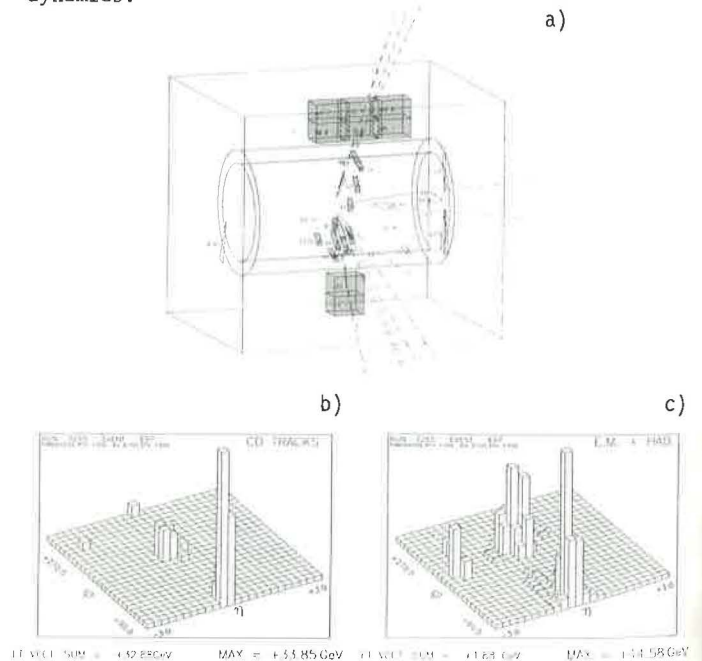


Fig. 9 A two-jet event seen in the UA1 detector (threshold of 1 GeV on transverse momentum for charged particles and on transverse energy); b) The corresponding transverse energy deposition in the calorimeters as a function of the polar angle (more precisely the pseudorapidity) and the azimuth.

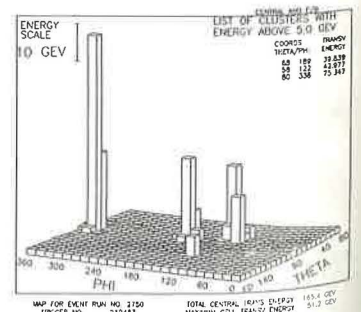


Fig. 10 Transverse energy deposition of a three-jet event in the UA2 calorimeter.

It appears then that the fundamental objects to study and to detect are less the single hadrons than the *jets*. This shift of emphasis would require fine-grain calorimetry. In that respect the segmentation of the UAI calorimeter is marginal. That of UA2 and CDF may even be insufficient, and more advanced designs will have to be considered such as those proposed for UAI⁴ or for the LEP or SLC detectors.

4. Experience with Existing Detectors

In addition to the three physics messages that we have outlined above, the experience with existing detectors has taught us fundamental lessons: the need for redundancy, the importance of visualization, and the necessity of hermetic energy measurement.

Because of the personal involvement of the author, the examples given will be taken from the UAI detector. Most of the conclusions, however, are general and apply equally well to UA2.

4.1 Redundancy

The need for redundancy can be exemplified by the W or Z⁰ detection. In 8×10^9 interactions, UAI has triggered 2×10^6 times, and selected 10^5 events among which fifty-five $W \rightarrow e^+ \nu$ and four $Z^0 \rightarrow e^+ e^-$ have been found. Thus extremely large rejection factors have to be reached.

In order to illustrate the methods used, we will describe the UAI selection⁴ of $W \rightarrow e^+ \nu$. Because of a clean situation, only "rough" criteria are needed. We require the observation of an electromagnetic cluster with a transverse energy larger than 15 GeV and negligible energy deposition in the hadron calorimeter as is expected for an electromagnetic shower. We request, in addition, that a fast isolated track points to this cluster and that no jet is observed back to back in azimuth.

These simple rules are sufficient to isolate 55 events. But how do we know that we have indeed extracted the $W \rightarrow e \nu$ events? That is where the redundancy of the UAI detector comes in.

Looking just at the missing transverse energy distribution (Fig. 11), we observe that 52 events have missing transverse energy significantly larger than the expected background. This is a clear indication that neutrinos are present.

We can also check that the charged particle behaves as an electron.

Figure 12 shows that the longitudinal profile of the shower is indeed that expected from an electron (both for the W candidates and the Z⁰ which are obtained in a similar fashion).

The position observed in the electromagnetic calorimeter should agree with the extrapolation from the central detector. This is the case (Fig. 13).

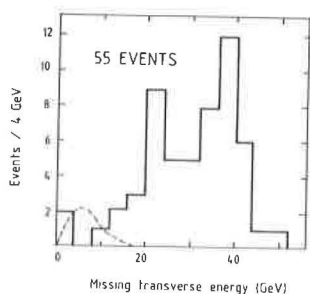


Fig. 11 Missing transverse energy distribution for the $W \rightarrow e \nu$ candidates (UAI).

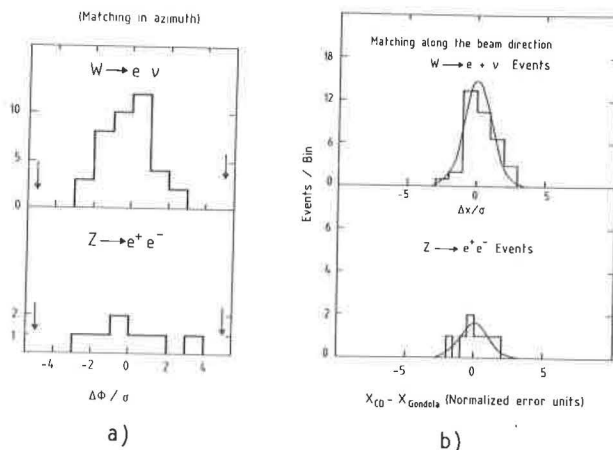


Fig. 12 Comparison of position for the W candidates: a) in azimuth; b) along the beam of the electron as measured by the electromagnetic calorimeter and by the central detector (UAI).

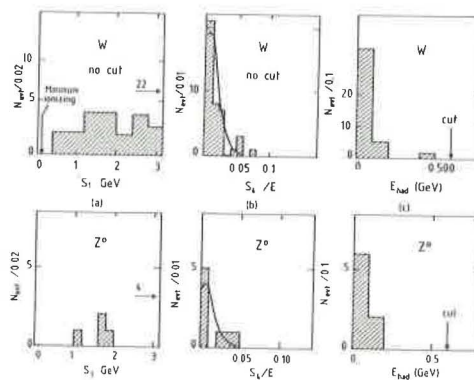


Fig. 13 Longitudinal profile of the electromagnetic shower for $W \rightarrow e \nu$ or $Z \rightarrow e^+ e^-$. a) Energy deposited in the first electromagnetic segment (minimum ionizing expected for non-interacting π); b) Ratio of energy deposited in the fourth electromagnetic segment to total energy (curve shows expectation); c) Energy deposited in hadron calorimeter.

Finally, the energy measured in the electromagnetic calorimeter should be compatible with that of the central detector. This is shown in Fig. 14, which displays the difference of the inverse of the energy and the inverse of the momentum, normalized by its

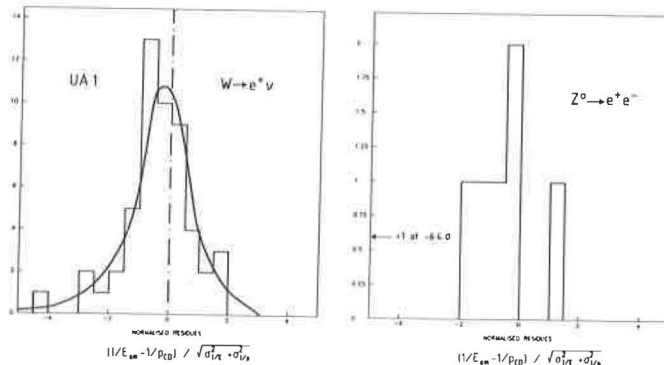


Fig. 14 Comparison of $1/E$ and $1/p$ of the electrons as measured in the electromagnetic calorimeter and in the central detector (UAI).

error. The slight deviation from a Gaussian expected (solid curve) from internal or external bremsstrahlung of the electrons is even observed!

Therefore, the redundancy of the UAl detector allows extremely convincing arguments of the observation of events of the type $W \rightarrow e\nu$ to be put forward. The identification of top jets will presumably be more difficult and will require the use of all the tools described above at the selection stage and not only as *a posteriori* checks.

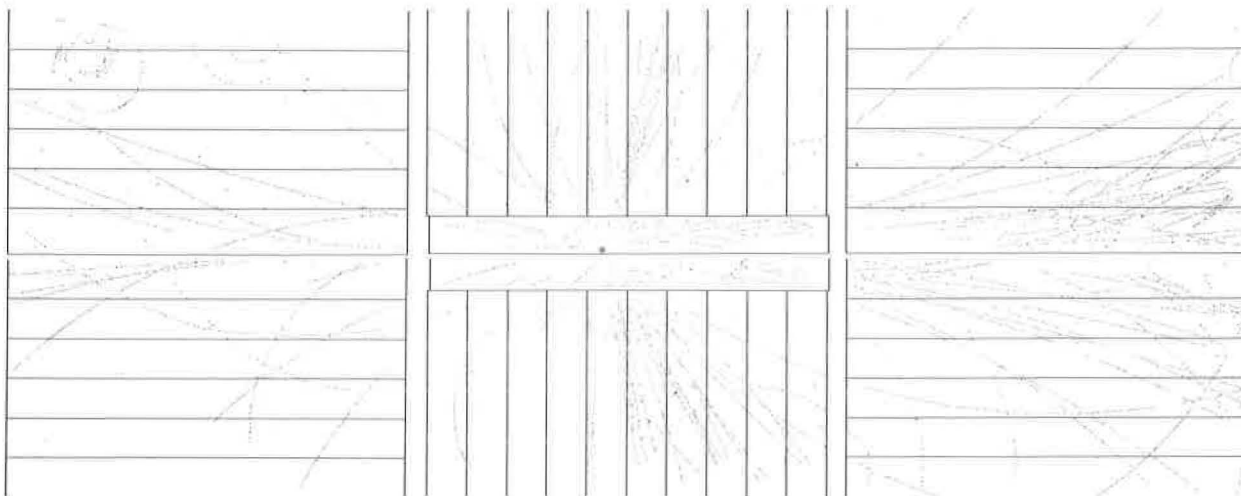


Fig. 15 A two-jet event (the same as in Fig. 9) as observed in the UAl central detector.

the magnetic field allows irrelevant low- p_T particles to be discarded.

The presence of jets requires a good two-particle resolution leading to a large number of cells. This is reasonably done by the UAl central detector. On the other hand, the UAl calorimeter is quite insufficient.

A final reason for visualization is that it is very useful for rare events to follow the interesting particles all through their lifetime in order to reject artefacts due to interactions, accidental overlap, decays, etc. Figures 16a and b show, for instance, the residuals in the central detector of the two muons for a Z^0 event. They can be contrasted clearly with a muon candidate in another event which is obviously a decay in flight (Fig. 16c).

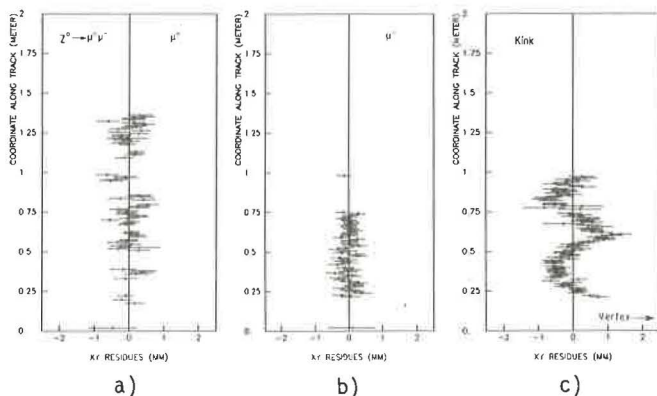


Fig. 16 a), b) Residuals of a circle fit to the μ^+ and μ^- trajectories in the UAl central detector for a $Z^0 \rightarrow \mu^+ \mu^-$ event. c) Similar residuals for an obvious decay.

4.2 Visualization

We have also found it extremely useful to have a great redundancy in the central detector giving a "visual" picture of the complete event.

The first reason is that the events themselves are very complex (see, for instance, Fig. 15) with additional tracks due to secondary interactions, δ rays, and γ conversions. To have an overall picture of the events is helpful, especially since as explained above

4.3 Hermetic Closure

We have already stressed the importance of total (transverse) energy measurement for the detection of neutrinos. This requires a hermetic closure of the detector, which should capture energy over the greatest possible fraction of the 4π solid angle.

The calorimetry in the UAl detector goes down to an angle of 0.2° with respect to the beam. In this way, it is able to measure missing transverse energy with a typical r.m.s. of 3 to 4 GeV (Fig. 17).

In addition to detection of neutrinos, such a good "hermeticity" improves considerably the physics output. Let us give three significant examples.

When no neutrino is expected to be present, such as in $Z^0 \rightarrow \mu^+ \mu^-$ the requirement of zero missing transverse energy gives two constraints which allow, as in

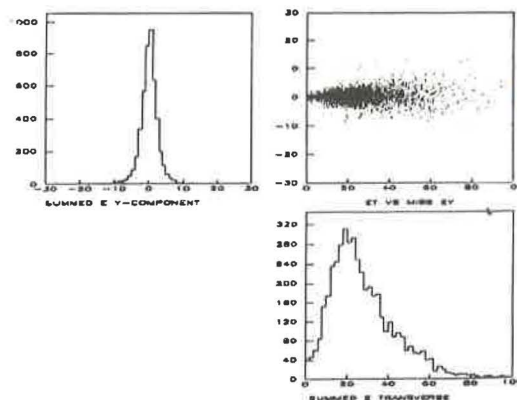


Fig. 17 Missing transverse energy in the y direction as a function of the scalar sum of transverse energy in the UAl detector for minimum bias events.

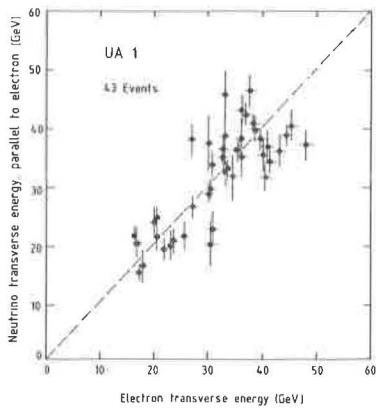


Fig. 18 The neutrino transverse energy balances the electron transverse energy (UA1).

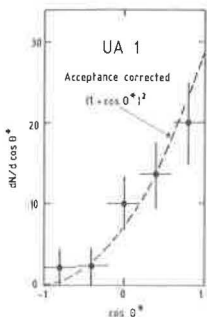


Fig. 19 The $W \cos \theta^*$ distribution, where θ^* is the angle of the electron (positron) with respect to the antiproton (proton) outgoing direction in the W centre of mass (UA1).

bubble chambers, improvement in the accuracy of the muon momenta and of the mass.

Figure 18 gives another example of the use of total energy measurement when a neutrino is produced. It shows that in the $W \rightarrow e\nu$ candidates the neutrino balances in azimuth the electron energy, giving a good indication that a *two-body process* is indeed observed.

An even more striking use of "hermeticity" is the possibility of solving the ambiguity of the determination of the W longitudinal momentum. This quantity is the solution of a second-degree equation requiring that the momentum of the electron (completely measured) and the momentum of the neutrino (measured only in its transverse component) combine to give the W mass. In the UA1 experiment, for 60% of the cases, the W energy of one solution is too big to be compatible with the energy observed for the rest of the event and therefore only one solution exists. This allows, for these events, to go unambiguously to the W centre of mass and extract the $\cos \theta^*$ distribution, θ^* being the angle of the electron (positron) with respect to the antiproton (proton) outgoing direction in that frame. Such a distribution (Fig. 19) shows clearly that *parity is violated*, that the *spin* of the observed particle is one, and that its coupling is *compatible with V-A* (or $V+A$). This is the ultimate proof that indeed it is the *intermediate vector boson* which has been observed.

5. Challenges

In spite of their power, illustrated in the previous section, existing collider detectors face many challenges, some of them already present, some linked with the expected improvement of colliders.

5.1 Accuracy

The demands of a high-energy collider in terms of accuracy, two-particle resolutions and absolute calibration are quite high.

Looking first at charged-particle detectors we can give an idea of the magnitude of the problem by noting that a 1 m track of 50 GeV (with useful length ~ 80 cm) in a 7 kG magnetic field has a sagitta of only 350 μm . This indicates the need for fiducial marks or calibration beams. It has been suggested to use a UV laser beam ionizing the chamber gas by two-photon absorption⁶. However, to date, no reliable system has been implemented in an experiment. The two-particle resolution of the UA1 central detector will have also to be improved with pulse shaping.

As far as calorimeters are concerned, we have already stressed that a finer segmentation would be needed for all experiments. The core size of a jet is typically 0.1 rad (half width at half maximum around $E_T = 40$ GeV/c) around 90° . For good jet reconstruction the cell size should be of the same order of magnitude and located at a distance such that the hadronic shower size is comparable or smaller (~ 1.5 -2 m). Moreover, cracks lead to loss of energy and lack of "hermeticity". Such effects are present both in UA1 and in UA2. Moreover, a real jet calorimetry would require similar response for the electromagnetic and hadronic components of the showers. This is possible with uranium⁷.

Finally, the absolute calibration may be crucial. For instance, the UA1 + UA2 mass difference of W and Z is at present⁴ 12.1 ± 1.5 GeV, which is slightly outside the standard theory bounds⁸ of 10.8 ± 0.5 . A more precise measurement would be a crucial test for the standard model. This would require in turn very stable calorimeters with excellent calibration ($\sim 0.1\%$). The best candidates may be devices based on liquid argon or tetramethyl silane⁹.

5.2 Flavour Identification

In addition to detecting the jets, one would like to identify their nature ("flavour"). This topic is discussed in detail by Wiik¹⁰ at this conference.

We should like to stress the importance of micro-vertex detectors. Secondary vertices are expected when bottom or charm quarks are produced. The UA1 Collaboration⁹ are planning to install a high-pressure drift chamber with 16 wires, each having an accuracy of 25 μm . Combined with a small 1 mm thick beryllium vacuum chamber of 50 mm diameter, such a device will be able to see secondary vertices in a large fraction of the cases (more than 50% for $W \rightarrow t\bar{b}$ or Higgs $\rightarrow b\bar{b}$ with present estimates of lifetimes).

5.3 Luminosity

The challenges of luminosity are summarized in the talk of Loken¹¹ at this conference: superposition of events, pile-up in individual detecting elements, distortions due to positive ions, d.c. shift, etc. In general, one can get around these limitations by using a large enough number of cells. Inversely a given detector is limited: for instance the large drift gaps used in the UA1 central detector exclude operation above its design of a few 10^{30} cm^2/s , a value which may eventually be reached by the Sp \bar{p} S Collider.

Another important consequence of luminosity is the need for "smart" triggers. Already at 2×10^{29} cm^2/s , we feel the necessity of going from "local" triggers (e.g. local high- E_T deposition or muon track) to "global" triggers (such as $e + \text{jet}$ or $\mu + \text{jet}$). This requires rather flexible and complex systems based on powerful on-line computers (68000, 168E, etc.).

5.4 Size and Complexity

But, perhaps the most fundamental challenge faced by experiments at high-energy colliders is that of size and complexity.

We have seen that a large number of cells is necessary both for charged-particle detectors and calorimeters. One way to limit the cost and complexity is to use clever multiplexing schemes. The concept of the time projection chamber allowed UA1 to divide a 20 m^3 volume into 8×10^5 pixels with only 6200 wires, providing a picture of bubble chamber quality. A similar idea is needed to instrument fine-grain calorimeters. With cell sizes given above, a few times 10^4 elements are easily reached. This large number of cells requires good reliability. Continuous monitoring and detailed diagnostics with the help of minicomputers are becoming common practice.

Last, but not least, the size of the collaborations becomes worrying. The UA2 group consists of 50 physicists, UA1 of 130, some LEP collaborations have more than 250 physicists. At these sizes, the problems of organization are far from trivial. In particular, the productivity of a team of physicists is strongly dependent on the flow of information, and the balance between personal initiative and consistent group action may be delicate.

6. Conclusion: Prospects for a 20-40 TeV detector

Will a detector for a 20-40 TeV machine be a "monster" which will be difficult financially to build, and hard physically to maintain and to manage? We do not think so.

The main reason is the shift of emphasis outlined in Section 3 towards jets and calorimetry. The size of calorimeters increases typically logarithmically with energy, while their relative accuracy improves as $1/\sqrt{E}$. Calorimeters have, therefore, obvious advantages with respect to magnetic detectors, which have to increase in dimensions as \sqrt{E} in order to maintain a constant relative accuracy.

However, because of the match between shower size and jet size mentioned in Section 5.1, the calorimeters cannot be too close to the interaction region. In the 1.5-2 m region available one would obviously place a charged particle detector in a moderate magnetic field, which would mainly be used as a filter to tag low-energy particles. Figure 20, taken from the Proceedings of the DPF Workshop at Berkeley¹², shows a possible sketch of such a detector. This may be too conventional compared to the possibilities which will be opened up in ten years from now. It just shows that detectors for 20-40 TeV machines will not necessarily be "dinosaurs" and that the collaborations involved could be maintained at a manageable size.

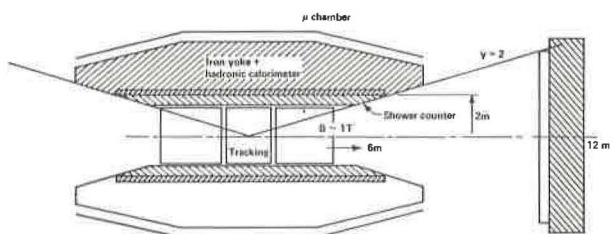


Fig. 20 A 20 TeV detector (from Ref. 12).

References

- UA1 proposal: A 4π solid-angle detector for the SPS used as a proton-antiproton collider at a centre-of-mass energy of 540 GeV, CERN/SPSC 78-06 (1978);
M. Barranco Luque et al., Nucl. Instrum. Methods 176, 175 (1980);
M. Calvetti et al., Nucl. Instrum. Methods 176, 255 (1980);
K. Eggert et al., Nucl. Instrum. Methods 176, 217, 223 (1980);
A. Astbury et al., Phys. Scr. 23, 397 (1981).
- B. Mansoulié, UA2 Collab., presented at XVIIth Rencontre de Moriond on Proton-Antiproton Collider Physics (La Plagne, March 1983), to be published;
A. Beer et al., The central calorimeter of the UA2 experiment at the CERN $p\bar{p}$ collider, to be published in Nucl. Instrum. Methods;
C. Conta et al., The system of forward-backward drift chambers in the UA2 detector, to be published in Nucl. Instrum. Methods;
K. Borer et al., Multitube proportional chambers for the location of electromagnetic showers in the CERN UA2 detector, to be published in Nucl. Instrum. Methods.
- Design report for the Fermilab Collider Detector Facility (CDF), Fermilab, August 1981.
- UA1 Collaboration: G. Arnison et al., Phys. Lett. 122B, 103 (1983);
G. Arnison et al., preprint CERN-EP/83-111, to be published in Phys. Lett. B.
G. Arnison et al., Phys. Lett. 126B, 398 (1983).
UA2 Collaboration: M. Banner et al., Phys. Lett. 122B, 476 (1983).
P. Bagnaia et al., Phys. Lett. 129B, 130 (1983).
- UA1 Collaboration: G. Arnison et al., Phys. Lett. 123B, 115 (1983).
G. Arnison et al., preprint CERN-EP/83-118, submitted to Phys. Lett. B.
G. Arnison et al., preprint CERN-EP/83-119, submitted to Phys. Lett. B.
UA2 Collaboration: M. Banner et al., Phys. Lett. 118B, 203 (1982).
P. Bagnaia et al., preprint CERN-EP/83-94, submitted to Z. Phys. C.
- H. Anderhub, M.J. Devereux and P.G. Seiler, Nucl. Instrum. Methods 166, 581 (1979) and 176, 323 (1980).
J. Bourotte and B. Sadoulet, Nucl. Instrum. Methods 173, 463 (1980).
M. Desalvo and R. Desalvo, Nucl. Instrum. Methods 201, 357 (1982).
H. Hilke, Nucl. Instrum. Methods 174, 145 (1980).
- C. Fabjan et al., Nucl. Instrum. Methods 141, 61 (1977).
- W. Marciano, Standard electroweak theory, Talk given at the International Symposium on Lepton and Photon Interactions at High Energies, Cornell, USA, 1983, and references therein.
- UA1 Collaboration, A proposal to upgrade the UA1 detector in order to extend its physics programme, CERN/SPSC/83-48, SPSC/P92 Add.3, 21 August 1983.
- B. Wiik, Talk at this conference.
- S. Loken, Talk at this conference.
- Proc. 1983 DPF Workshop on Collider Detectors: Present Capabilities and Future Possibilities, Berkeley, 1983 (LBL, Berkeley, 1983).